Optimisation of location and dimension of SMC precharge in compression moulding process

Moo-Sun Kim, Woo Il Lee, Woo-Suck Han, Alain Vautrin

Optimisation of location and dimension of SMC precharge in compression moulding process

Moo-Sun Kim [a,b], Woo Il Lee [a], Woo-Suck Han [b,*], Alain Vautrin [b]

[a] School of Mechanical and Aerospace Engineering, Seoul National University, Seoul 151-742, South Korea
[b] Division SMS, LTDS/CNRS UMR 5513, Ecole Nationale Supérieure des Mines de Saint-Etienne, 42023 Saint-Etienne, France

The main goal of the present study is to optimise the precharge conditions such as the precharge location and dimensions that give significant effects on the mechanical performance of composite structures man-ufactured by the compression moulding process. As preliminary step of optimisation, we developed a manufacturing simulation program to predict the fibre volume fraction and fibre orientation. And cou-pled with this simulation program and a structural analysis program, a genetic algorithm (GA) is imple-mented to optimise the precharge conditions. The penalty function method and the repair algorithm are modified for handling constraints. The repair algorithm is applied to a symmetric structure and an arbi-trary shape structure to find optimal precharge conditions.

1. Introduction

The compression moulding process is a manufacturing process in which precharges containing chopped fibres are compressed in a mould. In many cases, SMC (Sheet Moulding Compound) in the form of a thin sheet is used. At the design step, the fibre state of the structure to produce is assumed to have a homogeneous fibre volume fraction and an isotropic fibre orientation at anywhere on the structure. This fibre's state changes due to the flow characteristics produced during the filling process. The mechanical properties of the final product are determined dominantly by this fibre state. Consequently, this non-uniform distribution of the fibre state induced by the fibre separation or the change of fibre orientation during the compression moulding process generates non-uniform mechanical properties of the final product.

Some principal process parameters, such as the cure time, the mould closing speed, the moulding pressure and the precharge specification (geometry, placement and size of precharge) affect the quality of the final product. Among them, the precharge specification is considered as direct parameter because it induces various flow patterns during the process. In the case of arbitrary loading conditions, the fibre state with a homogeneous fibre volume fraction and an isotropic fibre orientation may be optimal for the mechanical performance. To realise a homogeneous and isotropic fibre state, a precharge covering the entire mould surface must be placed in the mould. If the mould has a complex shape, making the precharge shape becomes complicated. Generally, in the compression moulding process, the shape of the precharge is supposed as simple as possible and a rectangular one is preferred.

In this study, both manufacturing process simulation and structural analysis were coupled to perform multi-objective optimisation. And the location and dimensions of a rectangular-shaped precharge are considered as design variables to maximise the structural performance.

The first part of the study was dedicated to the understanding of the compression moulding process and the mechanical properties of the produced materials. The generalised Hele-Shaw (GHS) model proposed by Folgar and Tucker [1] is taken for the flow analysis of the compression moulding process. Regarding the change of fibre volume fraction during the manufacturing process, the fibre separation due to matrix–matrix and fibre–fibre interactions was proposed by Yoo [2] and Hojo et al. [3,4]. They modelled the fibre separation from the equilibrium between the drag force and the network force on fibres so as to predict fibre fraction. Moreover, the non-uniform fibre orientation distribution is one of the main causes for non-uniform mechanical properties in the product. As for the method to determine the state of fibre orientation, Jackson et al. [5] suggested the fibre orientation distribution function and Advani and Tucker [6–8] predicted fibre orientation by using orientation tensors. Also, Park et al. [9] suggested a fibre orientation model considering the fibre separation effect. In order to predict the mechanical properties of a short-fibre composite based on

* Corresponding author. Tel.: +33 477 42 0189; fax: +33 477 42 0249.
E-mail address: han@emse.fr (W.-S. Han).

the fibre state, the properties of a unidirectional composite should be estimated first. Halpin–Tsai equation is the most popular model for predicting the properties of short-fibre composites and is used to estimate the mechanical properties of unidirectional composites [10]. And the final fibre orientation tensors obtained from the simulation of compression moulding processing are used for obtaining the average orientation on any point in the product [6]. For the structural analysis of plate, a DST (Discrete Shear Triangle) element [11] and a DRM (Discrete Reissner–Mindlin) element [12] are used for thin and thick plate based on Reissner–Mindlin assumptions.

Till now, the most of research works for compression moulding process are separately dealt with the flow simulation, the prediction of fibre state or the structural properties induced by the fibre state. There are some works on other manufacturing processes for the optimisation of processing conditions or the structural design to obtain optimal structural properties. The structural optimisation considering manufacturing process for autoclave moulding was studied [13–15]. Park et al. performed a simultaneous optimisation considering structural and process constraints for RTM process [16–18]. Some studies suggested the optimal processing conditions as melt temperature and filling time for injection moulding process to improve mechanical properties [19,20]. For compression moulding process, some works were done on the optimisation of mould heating design or precharge shape in order to minimise surface temperature variation and keep uniform flow to prevent weld-line without considering fibre states or structural properties [21–23]. Kim et al. [24] performed the optimal thickness design considering compression moulding process effects coupled with the structural design.

In this work, to maximise structural properties of the final product manufactured by compression moulding process, the processing conditions such as the location and dimension of precharge are considered as design variables in optimisation problem.

This paper presents at first a numerical simulation approach of the compression moulding process using SMC precharge linked with the structural analysis. After that, an optimisation process to find optimal precharge conditions such as its location and dimension is presented. As optimisation method, a genetic algorithm (GA) is implemented. Furthermore, the method to define the precharge location and dimension using a GA is presented. As technique for handling the constraints, a penalty function method and a repair algorithm, modified for optimisation problems, are proposed.

2. Analytical and numerical modelling of flow and structure

2.1. Flow modelling

For the GHS model used to analyse the compression moulding process, it is assumed that the material is incompressible and the inertia is negligible because the flow in the thickness direction is negligible. The flow of filling process is assumed to be two-dimensional. Due to the small thickness, only the variation of the shear stress in the thickness direction is taken into account in the momentum equation. The flow velocity is defined as the average in-plane velocity in the thickness direction of the material. From the continuity and momentum equations with the above assumptions, the governing equation can be obtained as follows:

$$\frac{\partial}{\partial x}\left(\frac{S}{h}\frac{\partial P}{\partial x}\right)+\frac{\partial}{\partial y}\left(\frac{S}{h}\frac{\partial P}{\partial y}\right)=\frac{\dot{h}}{h}, \tag{1}$$

where $P, h, \dot{h}$ are the pressure, the thickness, and the compression speed, respectively and S is defined as the flow conductance. For the numerical analysis of fluid flow in this study, the fixed grid method is applied. To define the calculation domain, and thus to obtain the flow front location, the volume-of-fluid (VOF) method is used [25]. To calculate a more exact pressure distribution in flow front elements, the FINE method is applied [26].

2.2. Fibre separation modelling

To explain non-uniform distribution of fibre volume fraction in the final product, the fibre separation should be considered. In a concentrated suspension such as SMC precharge with a high fibre volume fraction, the fibre motion in flow is interfered by neighbouring fibres due to the interaction between fibres. Thus, the reinforcing fibres may move at different speeds from the surrounding matrix. Due to the relative velocity between the fibres and the main flow, the initial homogeneous fibre volume fraction in precharge may become heterogeneous and thus make the final mechanical properties non-uniform. The network force, F_{nw}, which is defined as resultant of the frictional forces (Fig. 1) acting on the fibre at different contact points with the neighbouring fibres, acts as a resisting force and thus gives rise to the relative motion of fibres. The relative velocity of matrix to fibre, u_s, is defined as:

$$u_s = u_c - u_f, \tag{2}$$

where u_c is the matrix velocity and u_f is the fibre velocity. It can be assumed that the drag force on the fibre by the resin flow is balanced by the frictional force on the fibre. Therefore, the relative velocity can be determined by using the equivalence between the drag force and network force. And, the network force can be defined as the difference in the frictional force caused by the pressure variation acting on the fibre [2].

With u_f from Eq. (2), the fibre volume fraction (ϕ) can be estimated by integrating the mass conservation of fibre for a control volume ($V_{c.v}$) as in Eq. (3) assuming that the fibre content and the rate of fibre content change are constant

$$\frac{\partial \phi}{\partial t}V_{c.v}+\int_{c.s}\phi u_f\cdot\hat{n}\,d\Gamma=-\frac{\dot{h}}{h}\phi V_{c.v}. \tag{3}$$

2.3. Fibre orientation modelling

A compact and general description of the fibre orientation state is provided by the tensors defined as follows:

$$a_{ij}=\oint p_i p_j \psi(p)dp, \tag{4}$$

$$a_{ijkl}=\oint p_i p_j p_k p_l \psi(p)dp, \tag{5}$$

where the unit vector p_i for two-dimensional orientation is defined as $p_1 = \cos\theta$, $p_2 = \sin\theta$ [6]. Note that a_{ij} is symmetric and its trace is equal to the unity. The advantage of tensor representation is that

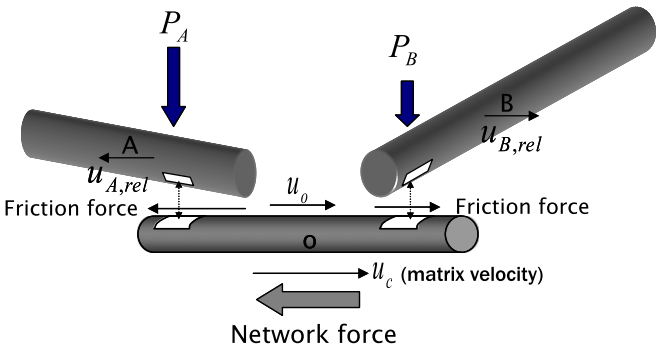

Fig. 1. Friction forces acting on fibres.

only a few numbers are required to describe the orientation state at any point in the space. For planar orientations, there are four components of a_{ij}, but only two are independent. An equation of single fibre motion that Folgar and Tucker suggested for a concentrated suspension [27], can be combined with the equation of continuity to produce an equation of change for the probability distribution function and/or the orientation tensor. The result for second-order orientation tensors is:

$$\frac{Da_{ij}}{Dt} = -\frac{1}{2}\left(\omega_{ik}a_{kj} - a_{ik}\omega_{kj}\right) + \frac{1}{2}\lambda\left(\dot{\gamma}_{ik}a_{kj} + a_{ik}\dot{\gamma}_{kj} - 2\dot{\gamma}_{kl}a_{ijkl}\right) + 2C_I\dot{\gamma}\left(\delta_{ij} - \alpha a_{ij}\right), \quad (6)$$

where δ_{ij} is Kronecker delta and α is equal to 2 for planar orientation. ω_{ij} and $\dot{\gamma}_{ij}$ are the vorticity and the rate of deformation tensors, respectively. C_I is an empirical constant called the interaction coefficient, and λ is a parameter related to the geometry of the fibre. To replace the fourth-order tensors with second-order tensors, hybrid closure approximation [6] is applied.

2.4. Structural analysis

By using the fibre volume fraction and fibre orientation tensors calculated from the processing simulation, the mechanical properties of a composite structure can be estimated. Firstly, the properties of unidirectional material are estimated using the Halpin–Tsai equation [10]. Next, the mechanical properties of the final product are calculated by considering the fibre volume fraction and taking an average of the unidirectional properties over all directions. For structural analysis, flat elements were employed. A typical flat element is subject to plane stress and plate bending action. Therefore, the stiffness matrix is formed by assembling the plane stress and plate bending stiffness matrices. Also, the plate bending stiffness matrix is composed of two different stiffness matrices, which are obtained from bending moments and transverse shear forces. In this investigation, a triangular three-node DRM element is used for a plate bending problem [12].

3. Optimisation of location and dimension of precharge

As previously mentioned, the precharge location and dimension can give significant effects directly on the fibre state according to various flow patterns. Therefore, the precharge location and dimension can be considered as design variables of optimisation problem to maximise the structural properties. It is assumed that the precharge has a simple shape, e.g. rectangular shape, and that the precharge size is given so as to keep a constant weight after filling. GA is implemented as optimisation method. And, to handle the constraints, the penalty function method and repair algorithm are modified.

3.1. Optimisation procedure

To predict quantitatively the fibre state to find optimal mechanical properties of the structure, a numerical filling simulation is performed. For this type of optimisation problems, it is not possible to calculate the gradient of the actual objective functions but to obtain an approximate gradient by finite differentiation. When the function f is continuously differentiable but the information about the gradient of f is either unavailable or unreliable, direct search method is useful because this method is derivative-free [28,29]. In this optimisation problem, GA is chosen as optimisation method. Precharge dimension and location are chosen as design variables, and it is necessary to generate a new mesh at every filling time step. Mesh regeneration has an advantage: the resolution of design variables can be modulated freely. For structural analysis, the initially generated mesh is used successively. To allocate the fibre states information from flow analysis to the nodes of the mesh for structural analysis, linear interpolation is implemented. Fig. 2 presents the flow chart of the optimisation.

3.1.1. GA

GA is based on the natural phenomena in which every individual of population tries to progress or survive in his natural environment. The natural phenomena simulated by GA are implemented as genetic operators, which process a set of design population during consecutive generations. The main operators are reproduction, crossover and mutation [30]. The reproduction phase involves the creation of a mating pool where superior design vectors are selected based on their fitness values. The crossover process is performed on the mating parent pool to produce new design vectors. The mutation operator alters the design vectors by substituting randomly some of the variables in them and provides a mechanism that not only explores the design space but also inherits some of the information of the previous design vector.

3.1.2. Definition of design variables

The first step in the development of GA is to generate the initial population. In the case of a multi-variable problem, to represent an individual of population, n variables are represented in binary form and attached in series as $\underbrace{101111}_{x_1}\ \underbrace{101101}_{x_2}\ \underbrace{010100}_{x_3}\ldots\underbrace{111001}_{x_n}$. In the optimisation problem, the design variables to represent the precharge location and dimension are expressed by a grid number in the x–y coordinate system and they were converted into binary form.

3.1.2.1. Precharge location. To define the precharge location, an x–y coordinate expression is implemented. As shown in Fig. 3(a), first, the development of the mould shape is projected on the x–y coordinate system. The domain for the centre of precharge is limited to the inside area of the mould, as in Fig. 3(b). In the example shown in Fig. 3, the possible range of the domain is from $l_{cx}/2$ to $l_{dx} - l_{cx}/2$ in the x-axis and from $l_{cy}/2$ to $l_{dy} - l_{cy}/2$ in the y-axis, where l_{dx}, l_{dy}, l_{cx}, l_{cy} are mould domain length in x-axis, in y-axis, precharge

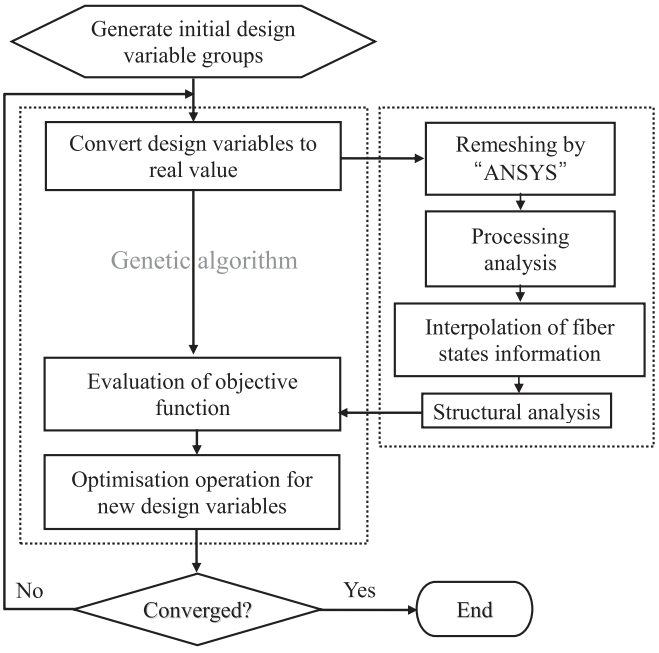

Fig. 2. Flow chart of precharge location and dimension optimisation.

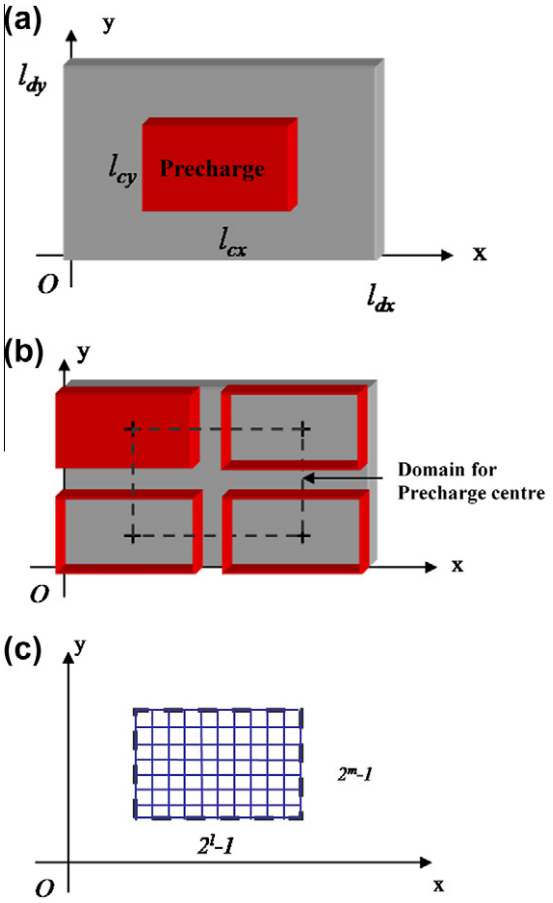

Fig. 3. Definition of domain for precharge centre and grids: (a) mould and precharge, (b) domain of precharge centre and (c) grids for precharge centre.

length in x-axis and in y-axis, respectively. Then, grids are generated in the domain of precharge centre on the x–y coordinate system, as in Fig. 3(c). The number of grids along the x-axis is $2^l - 1$, and $2^m - 1$ along the y-axis, where l and m are the integers for determining the resolution of the grids. One of the nodes in the grids is defined as the precharge centre. Applying this definition to GA, the grid numbers in x- and y-directions are implemented as design variables. With more grids, higher resolution of design vectors and more precise location become possible. Design vector, $\bar{x}$, for precharge location is defined as follows:

$$\begin{aligned}&\bar{x} = (x_1, x_2),\\ &x_1 : \text{Grid number of centre in } x\text{-axis}, \quad x_1 \in \{\text{integer } x_1 | 0 \leqslant x_1 < 2^l\},\\ &x_2 : \text{Grid number of centre in } y\text{-axis}, \quad x_2 \in \{\text{integer } x_2 | 0 \leqslant x_2 < 2^m\}.\end{aligned} \tag{7}$$

3.1.2.2. Precharge dimension. To define the precharge dimension as design vector, the precharge centre is considered to be located in the middle of mould in Fig. 4(a). Then, the development of mould shape is projected on the x–y coordinate system. Any applicable precharge dimension is possible in the range within the mould size. In the figure, the maximum possible precharge size is the same as the mould size. Then, within the maximum size, $2(2^n - 1)$ number of grids in the x-direction and $2(2^p - 1)$ number of grids in y-direction are generated on the x–y coordinate system, as in Fig. 4(b). Because the precharge has a symmetric shape, the actual number of grids to determine is $2^n - 1$ in the x-direction and $2^p - 1$ in the y-direction. The grid numbers in the x- and

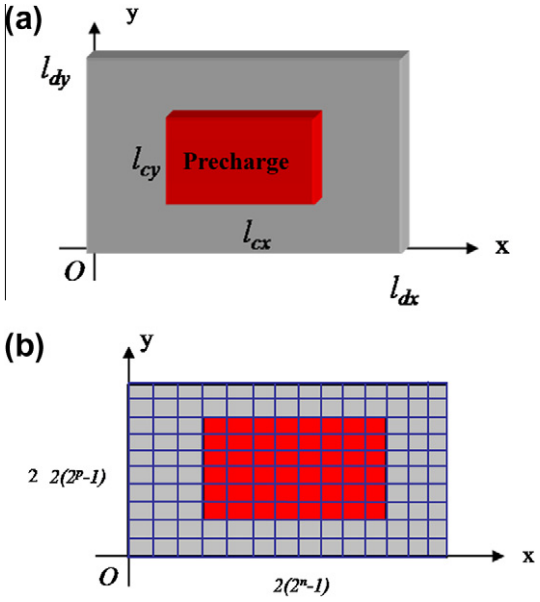

Fig. 4. Definition of domain for precharge dimension and grids: (a) mould and precharge and (b) grids for precharge dimension.

y-directions are expressed as a design vector to define optimal precharge dimension. Design vector for the precharge dimension is defined as follows:

$$\begin{aligned}&\bar{x} = (x_1, x_2),\\ &x_1 : \text{Grid number of dimension in } x\text{-axis}, \quad x_1 \in \{\text{integer } x_1 | 0 \leqslant x_1 < 2^n\},\\ &x_2 : \text{Grid number of dimension in } y\text{-axis}, \quad x_2 \in \{\text{integer} x_2 | 0 \leqslant x_2 < 2^p\}.\end{aligned} \tag{8}$$

3.1.2.3. Precharge location and dimension. Both precharge location and dimension can be considered simultaneously as design vectors, as shown in Fig. 5. In this case, because the precharge dimension is not determined in advance, the range of the centre of precharge location cannot be confined. Then, the entire mould area is defined as the possible region for the location of the precharge centre. The grids for the location are shown in Fig. 5(b). After setting one point of the grids as the precharge centre, other grids for precharge dimension are laid on the point, as shown in Fig. 5(c). Then, on the precharge dimension grids, precharge is placed with the dimension generated by dimension design vector. Design vector is defined as follows:

$$\begin{aligned}&\bar{x} = (x_1, x_2, x_3, x_4),\\ &x_1 : \text{Grid number of centre in } x\text{-axis}, \quad x_1 \in \{\text{integer } x_1 | 0 \leqslant x_1 < 2^l\},\\ &x_2 : \text{Grid number of centre in } y\text{-axis}, \quad x_2 \in \{\text{integer } x_2 | 0 \leqslant x_2 < 2^m\}\\ &x_3 : \text{Grid number of dimension in } x\text{-axis}, \quad x_3 \in \{\text{integer } x_3 | 0 \leqslant x_3 < 2^n\},\\ &x_4 : \text{Grid number of dimension in } y\text{-axis}, \quad x_4 \in \{\text{integer } x_4 | 0 \leqslant x_4 < 2^p\}.\end{aligned} \tag{9}$$

As shown in Fig. 5(d), if the precharge falls beyond the mould area, the process analysis cannot be carried out because the precharge must be completely located within the mould to keep the initial size for process simulation. To treat infeasible solutions (i.e. precharge partially or fully outside the mould), some techniques to handle constraints are needed.

3.2. Constraint handling techniques

A non-linear inequality constrained optimisation problem is formulated as

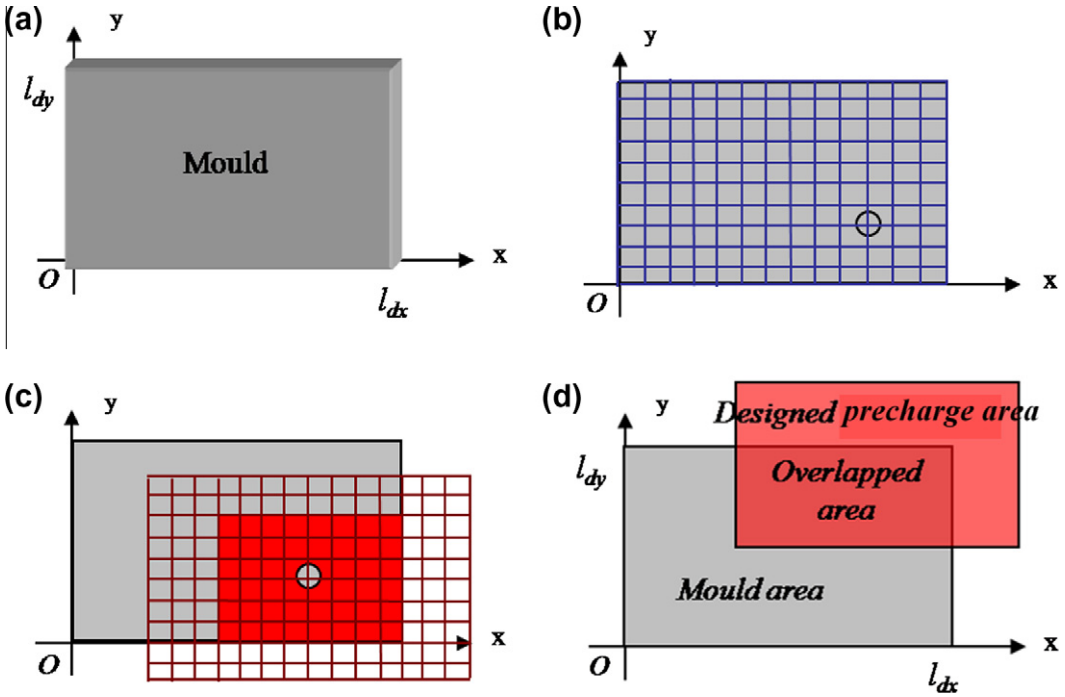

Fig. 5. (a) Mould shape and size. (b) Grids for precharge centre. (c) Grids for precharge dimension. (d) Location and dimension of infeasible design variable.

$$\begin{aligned} &\text{Minimise} \quad f(x), \\ &\text{subject to} \quad x \in \mathbf{S}, \quad g(x) \leqslant 0. \end{aligned} \tag{10}$$

$\boldsymbol{S}$ is defined as n-dimensional rectangle in R^n, i.e. $\boldsymbol{S} = \{x | l \leqslant x \leqslant u\}$, where l and u are the lower bound and upper bound of x, respectively. In general, the search space $\boldsymbol{S}$ consists of feasible and infeasible search spaces, $\boldsymbol{F}$ and $\boldsymbol{I}$, respectively. There are several methods for handling feasible and infeasible solutions [31–34]. The general method penalizes infeasible points and other methods reject and repair infeasible individuals. The rejection methods may work well when the feasible search space has a convex form and it constitutes a reasonable part of the whole search space. However, these methods have drawbacks in cases where all initial individuals are infeasible and the ratio between the sizes of $\boldsymbol{F}$ and $\boldsymbol{S}$ is small [34]. In GA, even an infeasible solution gives and transfers its partial information through operations. Therefore, the infeasible solutions should be allowed to provide information and not just be thrown away. Excluding the rejection methods, this study applies the penalty method and the modified repair algorithm to handle infeasible solutions.

3.2.1. Penalty method

Penalty method is one of the most popular approaches in GA. The approach assumes that

$$eval(\bar{x}) = f(\bar{x}) - p(\bar{x}), \tag{11}$$

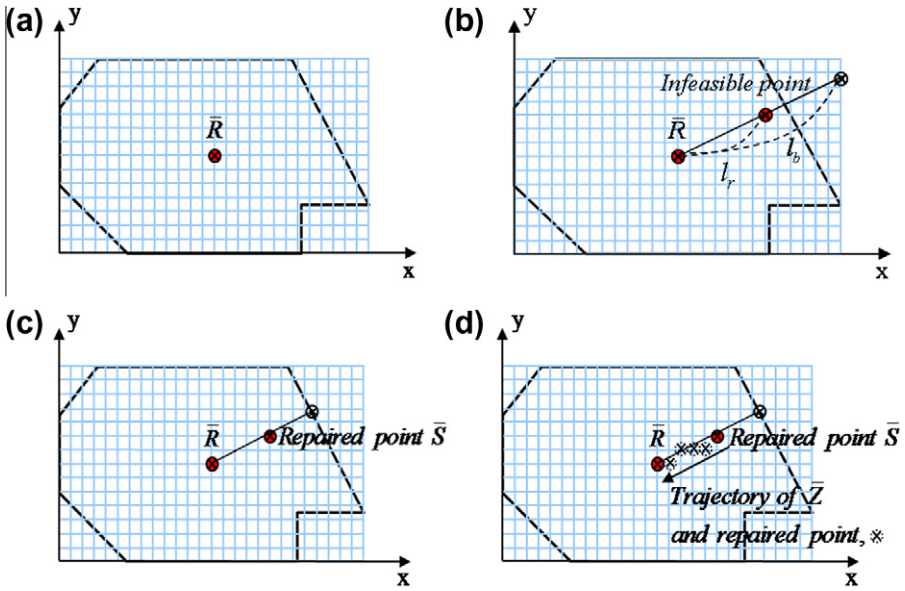

Fig. 6. Repair procedure for renewing the precharge centre.

where $p(\bar{x})$ represents a penalty function for infeasible individual in maximisation problem. The key point of this method is how to define the penalty function. The relationship between an infeasible individual and the feasible part of the search space plays a significant role in penalizing such infeasible individuals. In this study, the ratio between the precharge size overlapping the mould and the initial size is considered to present the penalty term as the distance from the feasible solution domain [35]. Therefore, the penalty function is defined as $p(\bar{x}) = 1 - \frac{Area_{overlapped}}{Area_{designed}}$.

The optimisation problem at hand is considered to be a stiffness maximisation problem. To maximise the stiffness, the maximum displacement of the structure under the given loading conditions should be minimised. For convenience, this displacement minimisation problem is converted into a maximisation problem by taking the inverse of the displacement

$$f(\bar{x}) = \frac{1}{d}, \quad d : displacement. \tag{12}$$

It is impossible to evaluate the objective function f when an individual is in the infeasible solution domain, because the process analysis with an infeasible precharge condition cannot be performed. In this case, f is set as 0. In order to prevent the evaluation function from having a negative value, an additional value, 1, equal

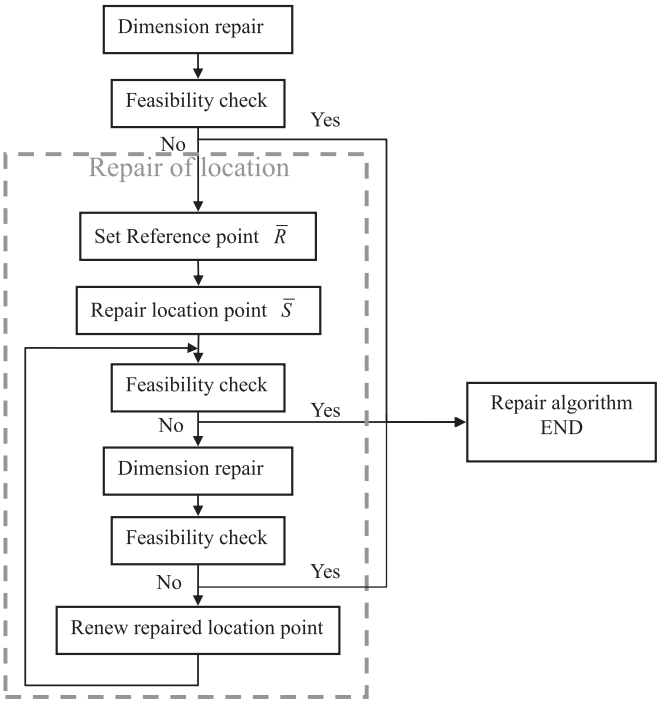

Fig. 7. Flow chart of repair algorithm for precharge location and dimension optimisation.

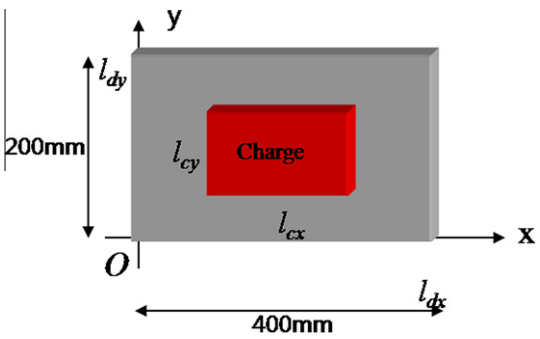

Fig. 8. Mould dimension for test function.

Table 1
Conditions for GA.

Population size	20
Maximum generation number	30
Crossover probability	0.8
Mutation probability	0.05

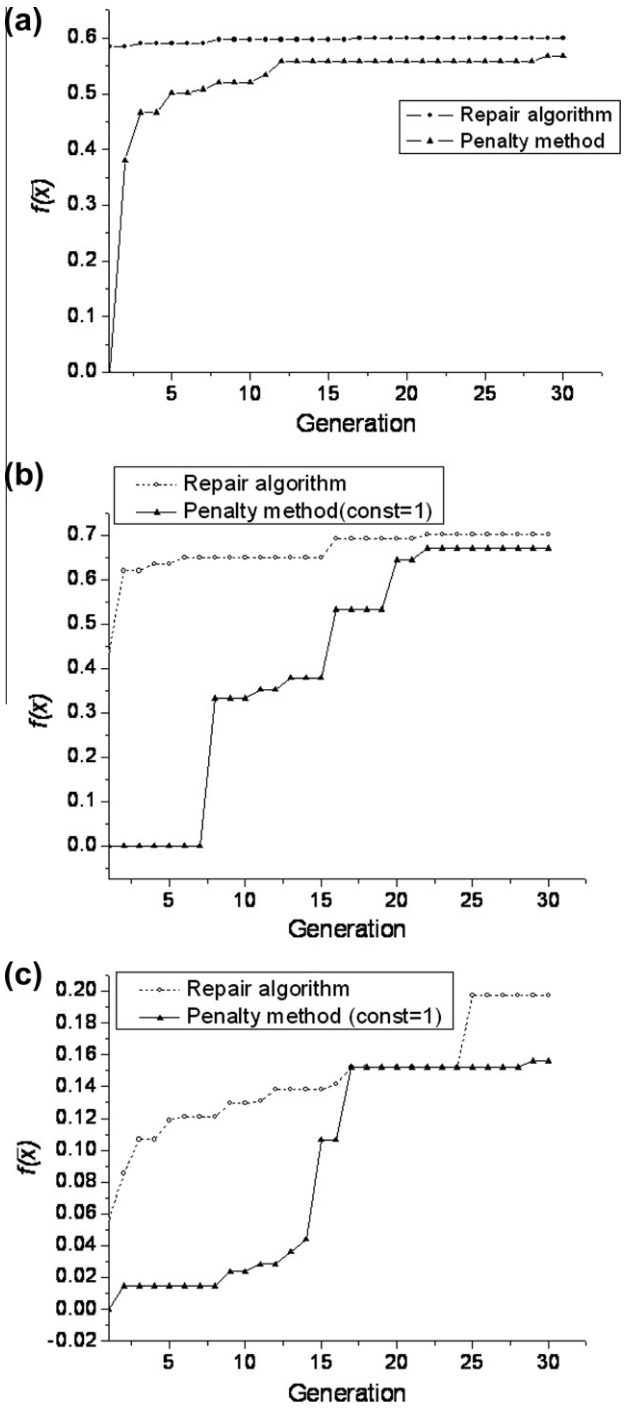

Fig. 9. Convergence test of repair algorithm and penalty method for (a) test function 1, (b) test function 2 and (c) test function 3.

to the maximum penalty value, was added to f. Consequently, the evaluation function is redefined as given as

$$eval(\bar{x}) = Const + f(\bar{x}), \quad if\ \bar{x}\ is\ feasible,$$
$$eval(\bar{x}) = Const \cdot \frac{Area_{overlapped}}{Area_{designed}}, otherwise. \tag{13}$$

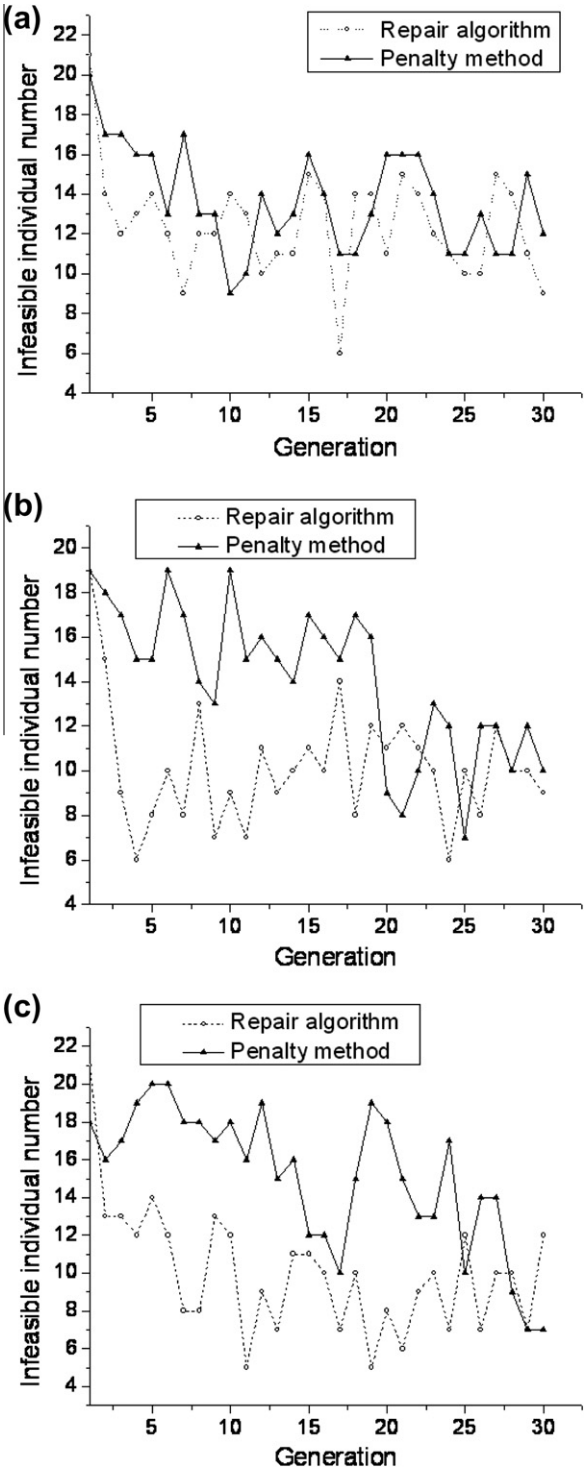

Fig. 10. Evolution of number of infeasible individuals for (a) test function 1, (b) test function 2 and (c) test function 3.

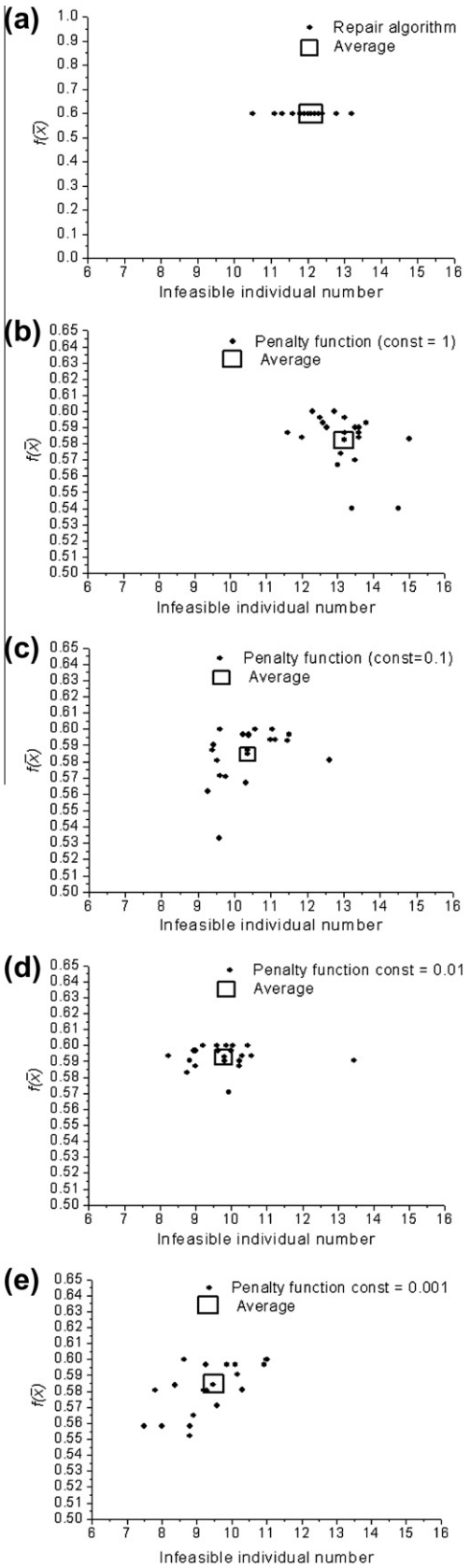

Fig. 11. Distribution of values of test function 1 and averaged number of infeasible individuals with 20 trials obtained by (a) repair algorithm, (b) penalty method (*Const* = 1), (c) penalty method (*Const* = 0.1), (d) penalty method (*Const* = 0.01) and (e) penalty method (*Const* = 0.001).

Table 2
Precharge material properties and processing conditions.

Initial fibre volume fraction	30%	Fibre tensile modulus	72.5 GPa
Fibre length	25 mm	Fibre shear modulus	30 GPa
Fibre bundle diameter	2.5 mm	Fibre Poisson ratio	0.2
Compression speed	1 mm/s	Resin tensile modulus	2.62 GPa
Viscosity	500 Pa s	Resin shear modulus	0.984 GPa
Initial fibre orientation	Random	Resin Poisson ratio	0.32
Proportionality constant κ	0.5	Interaction coefficient C_I	0.04

The closer the precharge size falls within the feasible solution domain, the higher becomes the evaluation function value. For penalty method, a scaling scheme is used to redefine the objective function, f. The values of the original function are converted by adding the quantity $C = 0.1f_h - 1.1f_l$ to each function value, where f_h and f_l are the highest and lowest values, respectively. Each new value is then divided by $D = f_h + C$ and the scaled function f_i', is defined as follows:

$$f_i' = \frac{f_i + C}{D}. \tag{14}$$

3.2.2. Repair algorithm

Repair algorithms are popular for many combinatorial optimisation problems. A repaired individual can be used for evaluation only, and the original individual can be succeeded or be replaced by the repaired one in the next generation. Various types of repair algorithm can be applied depending on the type of optimisation problem. Therefore, a specifically designed repair algorithm should be used for each particular optimisation problem [32–34,36,37]. For the optimisation of precharge location and dimension in this study, a repair algorithm is applied to handle the infeasible solution domain, in which the precharge falls beyond the mould area. Basically, the precharge dimension was repaired to maintain the initial shape as similarly as possible and the precharge location to be close to the feasible reference point [32]. The algorithm to repair the infeasible precharge location and dimension is composed of the following steps.

First, it checks whether the precharge size overlapping with the mould is the same as the original one. If they are the same, the evaluation function can be calculated for the original individual. If not, the following procedure is performed.

1. It checks to see if the precharge centre is inside the mould. If yes, the dimension design vector is repaired by decreasing the grid number in the x and y coordinate system by unit value, 1. Then, the feasibility constraint is checked. If the repaired design vector is within the feasible solution domain, the evaluation function is calculated. If not, the dimension design vector is repeatedly repaired until it falls beyond the dimension constraints.
2. If the design vector is not within the feasible solution domain, as shown by step 1, the location repairing procedure is performed in the next step.
3. The reference point $\overline{R}$ is set at the nearest node to the centre of grids for location optimisation, as shown in Fig. 6(a).
4. The point is found where the straight line from the reference point to the design vector in the infeasible area meets the grid boundary. Then, the ratio of the length l_r over the length l_b is

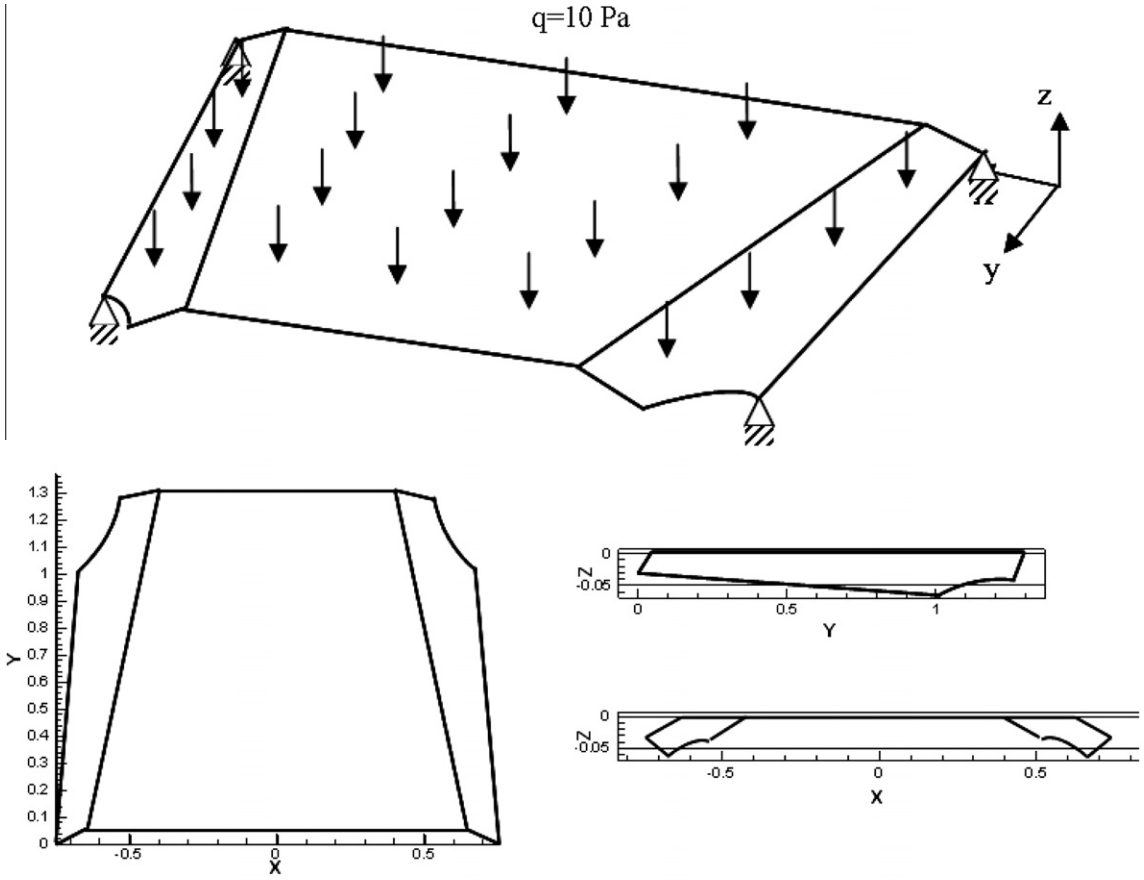

Fig. 12. Geometry and loading conditions of car-hood shaped structure.

calculated, where l_r is the length between the reference point and the repaired location design vector and l_b between the reference point and the infeasible point, as shown in Fig. 6(b).

5. The point where this straight line meets the mould boundary is found. Then, the node that is nearest to the point dividing the line by the previously obtained ratio is set as the repaired location design vector, $\overline{S}$, as shown in Fig. 6(c). Then, the feasibility is checked.
6. If feasibility is allowed, the evaluation is performed. If not, step 1 is repeated with the original precharge dimension.
7. If the repaired design vector is still not within the feasible domain, the nearest node point to the repaired location design vector, $\overline{Z}$, is renewed to approach to the reference point as $\overline{Z} = a\overline{S} + (1-a)\overline{R}$, where a is a constant between 1 and 0.
8. At the new repaired location design vector, step 1 is repeated with the original precharge dimension. Until a feasible individual is found by repairing, step 7 and step 1 are repeated by reducing a by 0.1 as shown in Fig. 6(d).

Through the above repair procedure, the initial infeasible design vector can be repaired to make it feasible. In the present study, the repaired individual replaces the old infeasible one for GA operations. The overall procedure of the repair algorithm is illustrated in Fig. 7.

3.2.3. Verification of penalty method and repair algorithm

Test function is applied to verify and compare the efficiency of the two present methods: penalty method and repair algorithm. For example, the plate shown in Fig. 8 is considered. Instead of performing the process and structural analysis, three test functions are defined with four variables, $\overline{X} = (X_1, X_2, X_3, X_4)$, as follows.

Test function 1: $f(\overline{X}) = X_1 + X_2 + X_3 + X_4$.

Test function 2:

$$f(\overline{X}) = \left(\frac{1}{(X_1-0.13)^2+0.00055} + \frac{1}{(X_2-0.02)^2+0.00045} + \frac{1}{(X_3-0.15)^2+0.0005} + \frac{1}{(X_4-0.07)^2+0.0004} \right) \Big/ 10000.$$

Test function 3:

$$f(\overline{X}) = \frac{0.0001}{(X_1-0.14)^2 + (X_2-0.067)^2 + (X_3-0.18)^2 + (X_4-0.105)^2 + 0.0005},$$

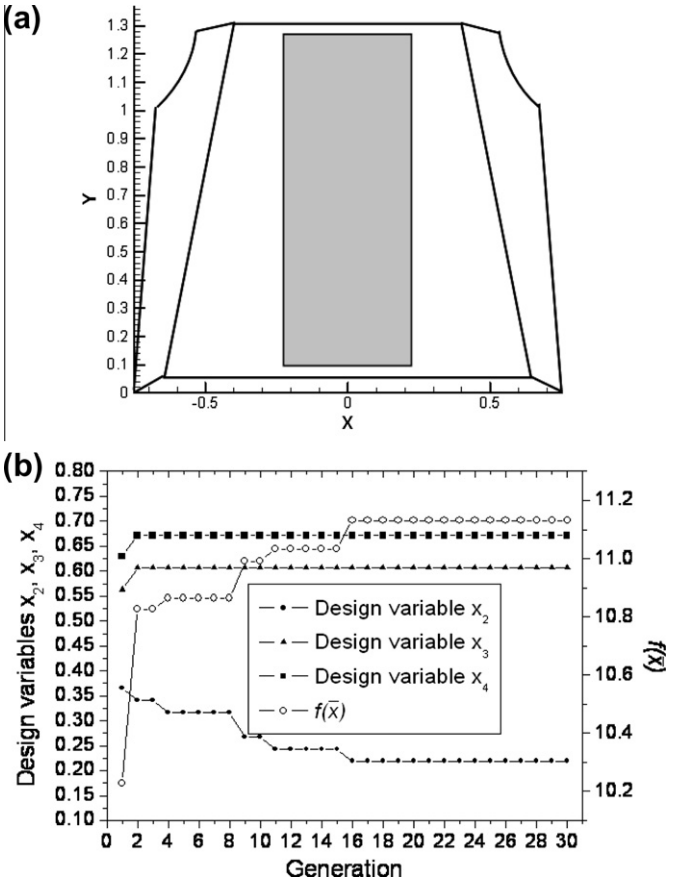

Fig. 13. (a) Optimal location and dimension of precharge. (b) Convergence of three design variables for precharge location and dimension optimisation.

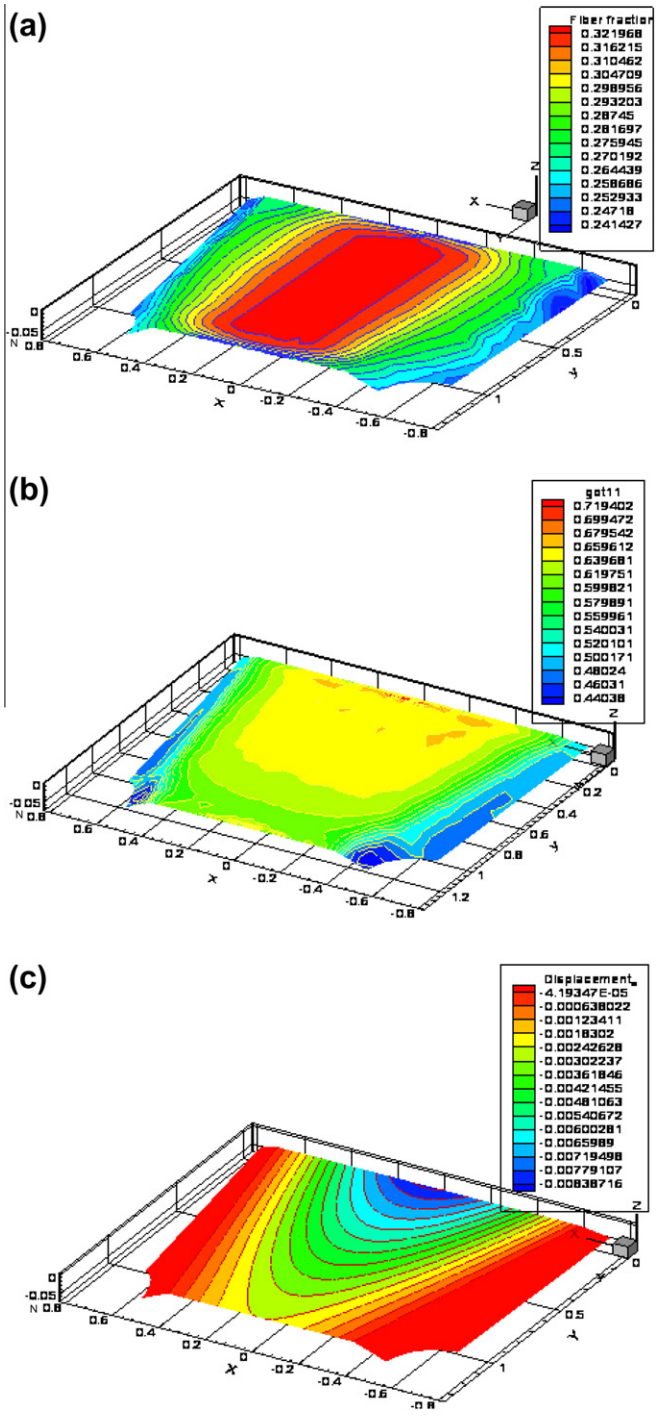

Fig. 14. (a) Distribution of fibre volume fraction. (b) Distribution of fibre orientation tensor a_{11}. (c) Displacement in z-direction.

where

$$X_1 = x_c(x_1), \quad X_2 = y_c(x_2), \quad X_3 = \frac{1}{2} l_{cx}(x_3), \quad X_4 = \frac{1}{2} l_{cy}(x_4),$$

x_c, y_c, l_{cx} and l_{cy} are the centre of precharge and precharge length in x-axis and in y-axis, respectively.

The numbers of grids for the design variables are set as $2^5 - 1$, $2^4 - 1, 2^5 - 1, 2^4 - 1$, respectively. In this case, 2^{18} solutions exist in the search space. Among them, there are 5804 feasible solutions.

The evaluation function for the penalty method is defined as

$$\begin{aligned} &\textit{Maximise } eval(\bar{X}) = Const + \bar{f}(\bar{X}), \quad \textit{if} \quad \bar{X} \textit{ is feasible design vector} \\ &eval(\bar{X}) = Const \cdot \frac{Area_{overlapped}}{Area_{Designed}}, \quad \textit{otherwise} \end{aligned}$$

where $\bar{f}(\bar{X})$ is scaled function.

For the repair algorithm, the evaluation function is defined as the test function, $f(\bar{X})$. Conditions for optimisation are given in Table 1.

Fig. 9 shows the convergence of test function value obtained by repair algorithm and penalty method ($Const = 1$) respectively. Fig. 10 shows the evolution of number of infeasible individuals. In both cases, most of the initially generated individuals are in the infeasible search space, but its number decreases through evolution. From Fig. 9, we can say that the repair algorithm converges to optimal solutions faster than the penalty method, because much more real numbers are evaluated by the repair algorithm than by the penalty method. It shows that the repair algorithm is more adapted to GA. Therefore, the repair algorithm has greater chances to find optimal solutions than the penalty methods. In Fig. 11, it depicts the distribution of values and the averaged numbers of infeasible individuals per generation with 20 trials of test function 1. As shown in Fig. 11, the repair algorithm does not miss finding an optimum solution during 20 tests with the variation of number of infeasible individuals. On the contrary, the penalty method has less chance to find optimal solutions. In the penalty method, there are many infeasible individuals according to *Const* value in the penalty function. It is clearly shown that the less becomes the *Const* value, the less the infeasible individual number becomes. However, the chance of finding an optimal solution with the penalty method does not increase with the *Const* value as efficiently as with the repair algorithm.

4. Example and results

The optimisation of precharge conditions is applied to a symmetric structure and an arbitrary and unsymmetrical shaped structure in 3D. In fact, as well as precharge conditions, other constraints should be also considered such as air-void or weld-line formation during the manufacturing process. However, in these examples, it is assumed that air-void can be removed through the vent and the fibre orientation represents the weld-line

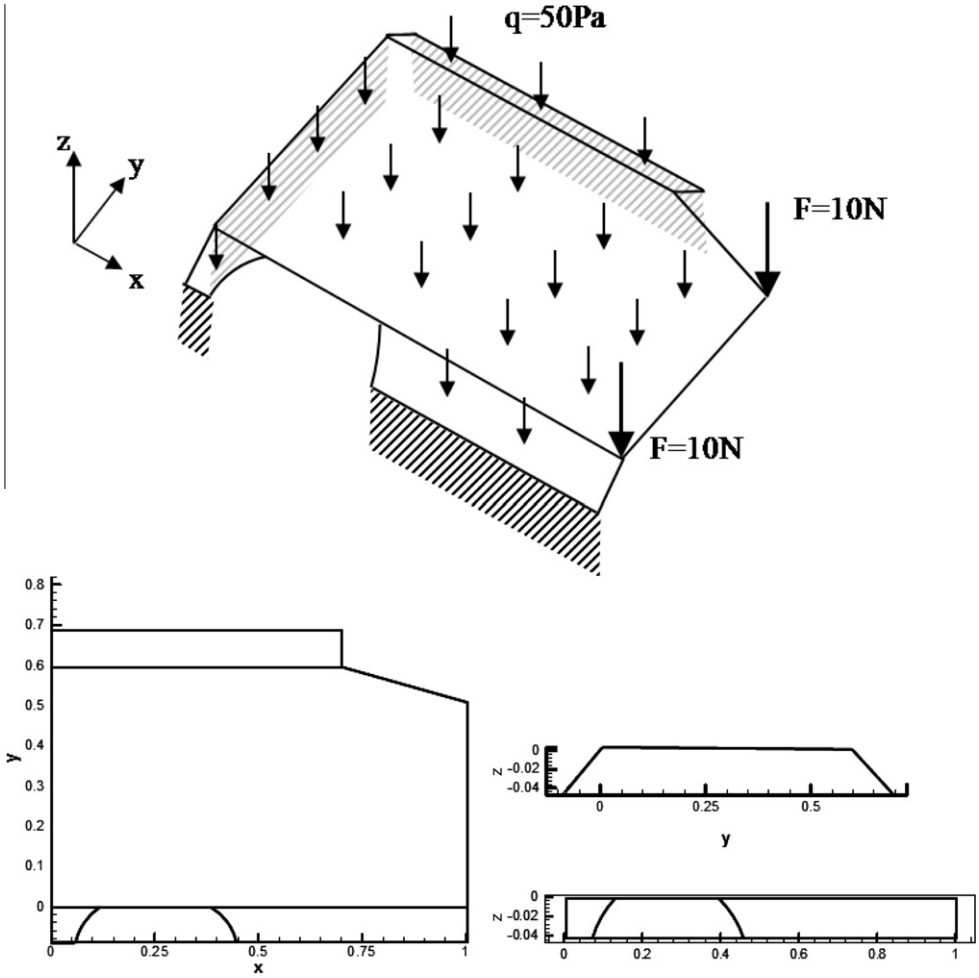

Fig. 15. Geometry and loading conditions of an arbitrary shaped structure.

characteristics. The material properties of the precharge and processing conditions are listed in Table 2.

The first example is the car-hood shaped structure. This structure has a symmetric shape, and two dimension and only one location (in y-axis) variables are considered. The geometry of the structure and loading conditions are shown in Fig. 12. The objective function and constraints are defined as follows:

$$\bar{x} = (x_2, x_3, x_4),$$

$$\text{Maximise} \quad f(\bar{x}) = \frac{1}{d}, \quad d: \text{ maximum displacement}$$

$$\text{Subject to design constraints } 0 \leqslant x_c(x_2) \leqslant l_{dx},$$

$$0 \leqslant \frac{1}{2} l_{cx}(x_3) \leqslant \frac{1}{2} l_{dx}, \quad 0 \leqslant \frac{1}{2} l_{cy}(x_4) \leqslant \frac{1}{2} l_{dy},$$

$$0.3 \leqslant \frac{Area_{Designed}}{Area_{structure}} \leqslant 0.7 \text{ and } \frac{Area_{Overlapped}}{Area_{Designed}} = 1.$$

The optimised precharge conditions for this problem and the searching procedure are shown in Fig. 13. The distribution of fibre volume fraction and fibre orientation tensors calculated by flow analysis and structural analysis with the optimised precharge conditions is shown in Fig. 14.

The structure considered as the second example has an arbitrary shape as shown in Fig. 15 and 4 variables are needed to be optimised.

The objective function and constraints are defined as follows.

$$\bar{x} = (x_1, x_2, x_3, x_4),$$

$$\text{Maximise } f(\bar{x}) = \frac{1}{d} d: \text{ maximum displacement}$$

$$\text{Subject to design constraints } 0 \leqslant x_c(x_1) \leqslant l_{dx},$$

$$0 \leqslant y_c(x_2) \leqslant l_{dy}, \quad 0 \leqslant \frac{1}{2} l_{cx}(x_3) \leqslant \frac{1}{2} l_{dx},$$

$$0 \leqslant \frac{1}{2} l_{cy}(x_4) \leqslant \frac{1}{2} l_{dy}, \quad 0.3 \leqslant \frac{Area_{Designed}}{Area_{structure}} \leqslant 0.7 \quad \text{and}$$

$$\frac{Area_{Overlapped}}{Area_{Designed}} = 1.$$

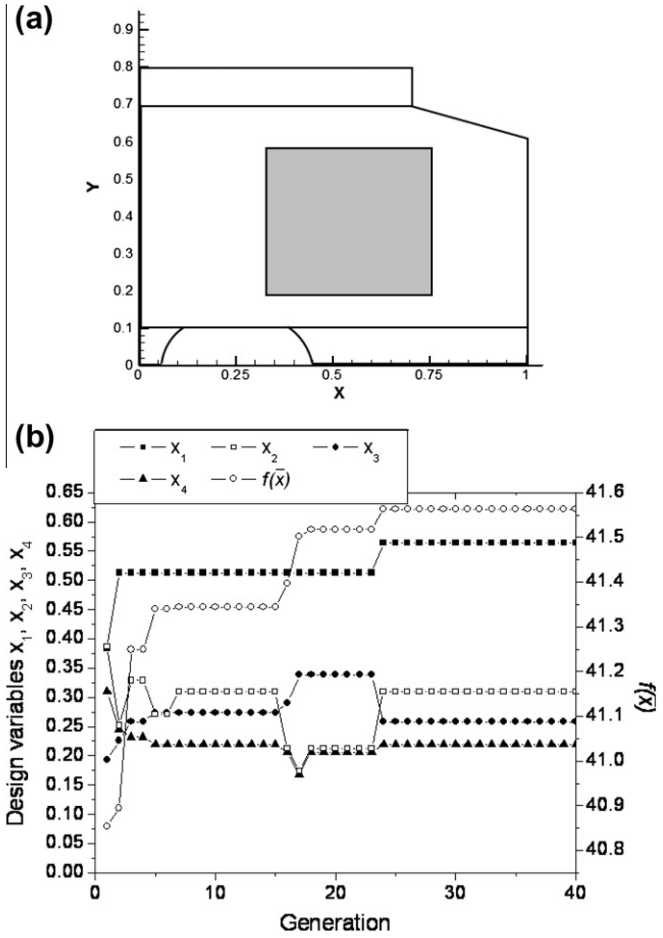

Fig. 16. (a) Optimal location and dimension of precharge. (b) Convergence of four design variables for precharge location and dimension optimisation.

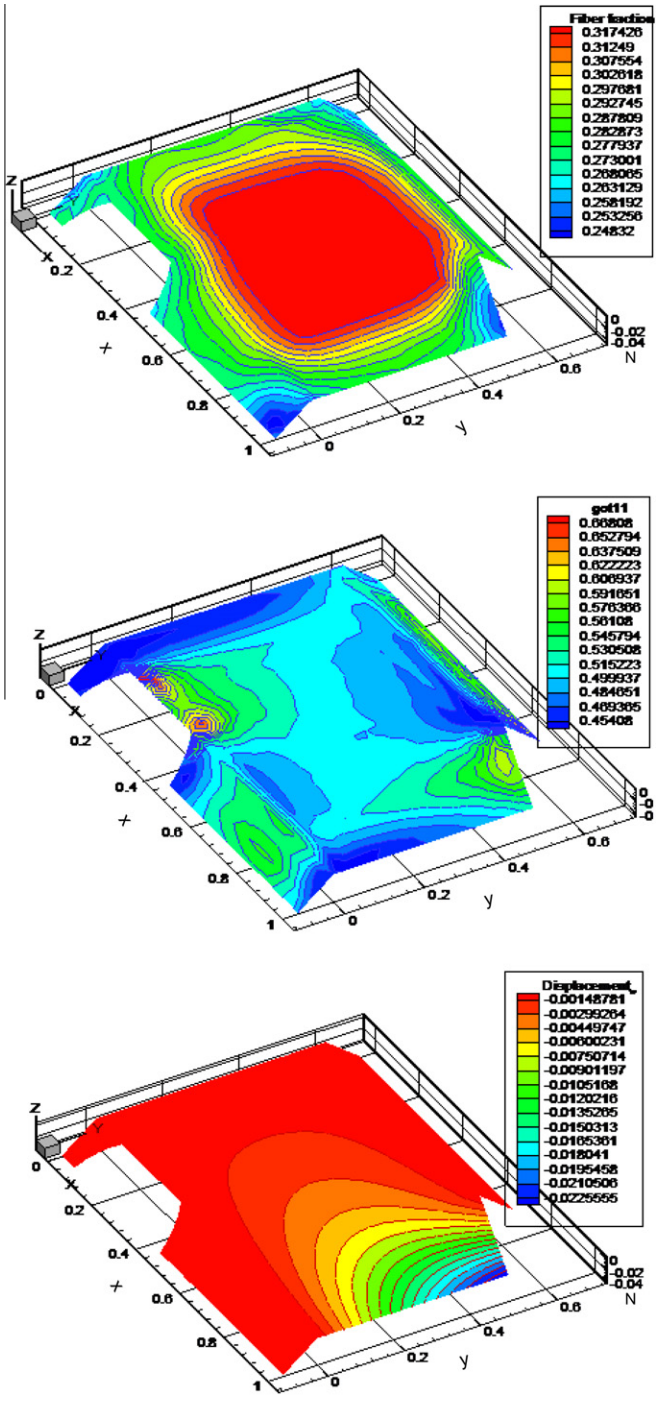

Fig. 17. (a) Distribution of fibre volume fraction. (b) Distribution of fibre orientation tensor a_{11}. (c) Displacement in z-direction.

The obtained optimised precharge conditions for this problem and the searching procedure are shown in Fig. 16. Also, the distribution of fibre volume fraction and fibre orientation tensors calculated with the optimised precharge conditions is shown in Fig. 17.

From the results of examples, the repair algorithm is found to be as effective as the penalty function method for handling constraints because the repair algorithm deals with the population in which every individual is feasible and no individual is thrown away. The modified repair algorithm in this study was effective for a structure with simple geometry. But it needs still other modifications for structures with a complex geometry, e.g. a structure with holes.

5. Conclusions

The optimisation of precharge conditions in compression moulding process was studied. To define the location and dimension of the precharge as a design vector, the grids were implemented to determine its location and size. To treat this optimisation, the whole search field of the design vector was divided into two spaces, the feasible and infeasible search spaces, because of the correlations of the design variables and constraints. To handle these constraints, penalty function method and repair algorithm were implemented. In the penalty function method, the penalty term was defined as the ratio between the precharge size overlapped on the mould and the original mould size. Concerning the repair algorithm, a modified repair algorithm was suggested. The optimisation results of both methods applied to test functions were compared and it was verified that the modified repair algorithm showed better performance. The repair algorithm is problem-dependent and it is necessary to be modified due to the problem characteristics. In this study, only structures with simple geometry were considered. However, for a structure with complex geometry, the repair algorithm would need to be modified. In addition to complex shaped structure, multi-precharge conditions can be another problem to consider. These conditions need the use of more than two precharges with different locations and dimensions. And further investigation of this case can be suggested based on the methodology proposed in this study.

References

[1] Folgar F, Tucker III CL. A model of compression mould filling. Polymer Engineering and Science 1983;23(2):69–73.

[2] Yoo YE. A Study on the analysis of compression moulding process of composite material structures. PhD thesis, Seoul: Seoul National University; 1997.

[3] Hojo H, Nagatsuka C, Kim EG, Tamakawa K. Separation of matrix and fibres during moulding of long reinforced–reinforced thermoplastics. In: Composites' 86: recent advances in Japan and the United States, proceedings of the third Japan–US conference on composite materials, Tokyo, 23–25 June; 1986. p. 605–12.

[4] Hojo H, Kim EG, Yaguchi H, Onodera T. Simulation of compression moulding with matrix–fibre separation and fibre orientation for long reinforced–reinforced thermoplastics. Int Polym Process III 1988:54–61.

[5] Jackson WC, Tucker CL, Advani SG. Predicting the orientation of short fibres in thin compression moldings. J Compos Mater 1986;20:539–57.

[6] Advani SG, Tucker III CL. The use of tensors to describe and predict fibre orientation in short fibre orientation in short fibre composite. J Rheol 1987;31(8):751–84.

[7] Advani SG, Tucker III CL. A numerical simulation of short fiber orientation in compression molding. Polym Compos 1990;11(3):164–73.

[8] Advani SG, Tucker III CL. Closure approximation for three-dimensional structure tensors. J Rheol 1990;34(3):367–86.

[9] Park CH, Lee WI, Yoo YE, Kim EG. A study on fiber orientation in the compression molding of fiber reinforced polymer composite material. J Mater Process Technol 2001;111:233–9.

[10] Halpin JC, Kardos JL. The Halpin–Tsai equation: a review. Polym Eng Sci 1976;16(5):344–52.

[11] Batoz JL, Lardeur P. A discrete shear triangular nine dof element for the analysis of thick to very thin plates. Int J Numer Methods Eng 1989;28:533–60.

[12] Zienkiewicz OC, Taylor RL, Papadopoulos P, Onate E. Plate bending elements with discrete constraints: new triangular elements. Comput Struct 1990; 35(4):505–22.

[13] Fine AS, Springer GS. Design of composite laminates for strength, weight, and manufacturability. J Compos Mater 1997;31(23):2330–90.

[14] Manne PM, Tsai SW. Design optimization of composite plates: Part II-structural optimization by plydrop targeting. J Compos Mater 1998;32(6): 572–98.

[15] Manne PM, Tsai SW. Design optimization of composite plates: Part I-design criteria for strength, stiffness, and manufacturing complexity of composite materials. J Compos Mater 1998;32(6):544–71.

[16] Park CH, Lee WI, Han WS, Vautrin A. Weight minimization of composite laminated plates with multiple constraints. Compos Sci Technol 2003;63: 1015–26.

[17] Park CH, Lee WI, Han WS, Vautrin A. Multi-constraint optimization of composite structures manufactured by resin transfer molding process. J Compos Mater 2005;39(4):347–74.

[18] Park CH, Lee WI, Han WS, Vautrin A. Improved genetic algorithm for multidisciplinary optimisation of composite laminates. Comput Struct 2008;86:1894–903.

[19] Chang SH, Hwang JR, Doong JL. Optimization of the injection molding process of short glass fiber reinforced polycarbonate composites using grey relational analysis. J Mater Process Technol 2000;97:186–93.

[20] Yang YK. Optimization of injection molding process for mechanical properties of short glass fiber and polytetrafluoroethylene reinforced polycarbonate composites: a case study. J Reinforced Plast Compos 2006;25(12):1279–90.

[21] Barone MR, Caulk DA. Optimal thermal design of compression molds for chopped–fiber composites. Polym Eng Sci 1981;21(17):1139–48.

[22] Twu JT, Lee LJ. Simulation-based design of sheet molding compound (SMC) compression molding. Polym Compos 1994;15(5):313–26.

[23] Twu JT, Lee LJ. Application of artificial neural networks for the optimal design of sheet molding compound (SMC) compression molding. Polym Compos 1995;16(5):400–8.

[24] Kim MS, Lee WI, Han WS, Vautrin A, Park CH. Thickness optimization of composite plates by Box's complex method considering the process and material parameters in compression molding of SMC. Compos Part A 2009; 40(8):1192–8.

[25] Hirt CW, Nichols BD. Volume of fluid (VOF) method for the dynamics of free boundaries. J Comput Phys 1981;39:201–25.

[26] Kang MK, Lee WI. A flow-front refinement technique for the numerical simulation of the resin-transfer moulding process. Compos Sci Technol 1999;59:1663–74.

[27] Folgar F, Tucker III CL. Orientation behavior of fibres in concentrated suspensions. J Reinforced Plast Compos 1984;3:98–119.

[28] Lewis RM, Torczon V, Trosset MW. Direct search methods: then and now. J Comput Appl Math 2000;124:191–207.

[29] Carson Y, Maria A. Simulation optimization: methods and application. In: Proceedings of the 1997 winter simulation conference, Atlanta. GA; 1997. p. 118–26.

[30] Goldberg DE. Genetic algorithms in search, optimisation and machine learning. Addison Wesley; 1989.

[31] Deb K. An efficient constraint handling method for genetic algorithms. Comput Methods Appl Mech Eng 2000;186:311–38.

[32] Michalewicz Z, Nazhiyath G. Genocop III. A Co-evolutionary algorithm for numerical optimisation problems with nonlinear constraints. In: Proceedings of the second IEEE ICEC. Piscataway, NJ; 1995. p. 647–51.

[33] Michalewicz Z, Dasgupta D, Le Riche RG, Schoenauer M. Evolutionary algorithms for constrained engineering problems. Comput Eng 1996;30(4): 851–70.

[34] Coello Coello CA. Theoretical and numerical constraint-handling techniques used with evolutionary algorithms: a survey of the state of the art. Comput Methods Appl Mech Eng 2002;191:1245–87.

[35] Richardson JT, Palmer MR, Liepins G, Hilliard M. Some Guidelines for genetic algorithms with penalty functions. In Proceedings of the third international conference on genetic algorithms. Los Altos. CA; 1989. p. 191–7.

[36] Renner G, Ekart A. Genetic algorithms in computer aided design. Comput Aid Des 2003;35:709–26.

[37] Michalewicz Z. A survey of constraint handling techniques in evolutionary computation method. In: Proceedings of the 4th annual conference on evolutionary programming. San Diego, CA; 1995. p. 135–55.